Proceedings of the 21st ICSMGE, Vienna, Austria, 14 – 19 June 2026. Pistrol, Adam & Schweiger (eds.)
Published by: ÖGG, Austrian Society for Geomechanics, Salzburg, Austria, ISBN 978-3-9503898-4-5
https://doi.org/10.53243/ICSMGE2026-1880

Gas barriers in geotechnical engineering: from deep geological disposal to engineered barriers/seals

Laura Gonzalez-Blanco, Enrique Romero
Civil and Environmental Department, Universitat Politècnica de Catalunya (UPC) and Geomechanics Group, International Centre for Numerical Methods in Engineering (CIMNE), Barcelona, Spain laura.gonzalez.blanco@upc.edu

ABSTRACT: Gas transport in geotechnical systems is a key challenge in various geotechnical engineering applications, especially in deep geological disposal and the design of engineered barriers and seals for the energy and environmental sectors. Understanding the performance of the materials against gas accumulation, pressurization and breakthrough pressure, as well as knowing the gas transport mechanisms through the barriers and the effective permeability, is crucial for ensuring long-term safety and functionality in these settings. The accumulation and transport of gas can compromise the integrity of containment systems by inducing hydro-mechanical damage, altering the host rock properties, and affecting the engineered barriers. Similarly, gas control is essential in engineered seals used in underground storage or remediation projects to prevent leakage and maintain the system's integrity under operational and post-closure conditions. This study explores, from an experimental viewpoint, several materials for gas barriers/seals, including compacted granular bentonite, composite systems (pellet/powder bentonite mixture), gas permeable barriers (sand/bentonite mixtures), and deep argillaceous indurated and plastic rocks. Laboratory experiments are used to evaluate their gas transport properties under varying stresses, stress histories, liquid saturation, and boundary conditions. A particular focus is placed on the interplay between material microstructure and gas transport phenomena, including self-sealing capability after re-saturation. The results provide valuable insights into the performance and mechanisms of a variety of gas barriers under complex conditions, offering a foundation for optimizing their design and extending their applications in geotechnical engineering.

KEYWORDS: Unsaturated soils, compacted engineered clay barriers, host rocks, gas transport, permeability, microstructure.

1 INTRODUCTION

Gas transport through clay-based materials is a key concern in environmental and energy geotechnics, particularly in the context of deep geological disposal (DGD) of radioactive waste. Gas is generated through several processes, including anaerobic corrosion of metallic components, radiolysis of porewater, and microbial activity, which can potentially lead to pressure build-up within the repository system. The accumulation of these gases may induce excessive pressures, leading to hydro-mechanical damage, pathway dilation, or even fracturing of the host rock and engineered barrier system (EBS), thus compromising their long-term containment function (Levasseur et al. 2024).

Clay-rich materials are widely used in multi-barrier systems due to their low permeability, radionuclide retention properties, and swelling capacity, which enables self-sealing of technological gaps, fractures, or preferential pathways (Marschall et al. 2024). However, gas migration through such low-permeability media can occur via different mechanisms depending on gas generation rates and hydro-mechanical boundary conditions, including diffusion of dissolved gas in porewater, two-phase flow, or dilation-induced flow along preferential pathways. Laboratory and field studies have shown that when gas increases, the transport can transition from diffusion-dominated to localized advective flow with potential structural damage (Ali et al. 2025; Gonzalez-Blanco & Romero 2024; Harrington et al. 2017; Llabjani et al. 2025).

The research team at the Geotechnical Laboratory of Universitat Politècnica de Catalunya (UPC) has conducted a comprehensive research program addressing gas transport phenomena in collaboration with three major European radioactive waste management agencies, NAGRA (Switzerland), ANDRA (France), and ONDRAF/NIRAS (Belgium), and the French Institute for Radiological Protection and Nuclear Safety (IRSN). This collaborative framework has enabled the investigation of a wide range of potential materials, both natural and engineered, and provided a unique opportunity to explore and compare gas transport mechanisms and self-sealing behavior under diverse hydro-mechanical boundary conditions. As a result, our laboratory has developed a broad and integrated understanding of the coupled processes governing gas transport and self-sealing in clay-rich environments.

Within the argillaceous host rocks for DGD, the studied materials include poorly indurated and plastic Boom Clay (potential host formation in Belgium; Gonzalez-Blanco & Romero 2024) and the indurated Opalinus Clay and Brown Dogger formations (the first one a potential host formation in the Swiss program; Senger et al. 2014, Senger et al. 2018). Their differing properties, including swelling pressure, stiffness, liquid permeability, and self-sealing capacity, provide valuable insight into how they affect gas transport and sealing performance (Gonzalez-Blanco et al. 2022).

Clay-based materials for EBSs, like granular bentonite, pellet/powder bentonite mixtures, and sand/bentonite mixtures, are also discussed in the paper. These engineered materials have been tailored for two main gas management strategies: (i) seals with a relatively high gas breakthrough pressure that rely on the swelling and self-sealing capacity of smectite-rich clays to restore hydraulic performance after gas invasion (Villar & Lloret 2008), and (ii) engineered gas-permeable barriers/seals that facilitate controlled gas dissipation at low gas breakthrough pressures while preserving low liquid permeability.

In the first EBS group, new typologies of bentonite forms, such as granular bentonite proposed in the Swiss concept (Müller et al. 2017) or composite bentonite systems, including powder/pellet bentonite mixtures adopted in the French concept (Mokni et al. 2023; Molinero-Guerra et al. 2016), have been proposed to limit potential damage by slightly reducing the breakthrough pressure compared to finer bentonites, while still acting as low-permeability and high swelling pressure barriers/seals (Ali et al. 2025).

The second EBS group involves designing sand/bentonite (S/B) mixtures with enhanced gas transport capacity to prevent excessive gas pressure build-up. Mixtures have been proposed with a dominant inert component (sand) compared to the swelling material. These mixtures have been implemented in Switzerland's engineered gas transport system (EGTS) concept using S/B with low bentonite content (20% dry mass). In particular, the GAST large-scale in situ test at the Grimsel Test Site (Switzerland), developed by NAGRA to demonstrate the

effective functioning of the gas permeable seal (Rüedi et al. 2012), has been complemented by supporting decimeter-scale mock-ups to study the effects of compaction layers on gas transport and sealing processes (Romero et al. 2023; Romero et al. 2024).

Following a similar gas-permeable seal concept, ANDRA has also examined S/B with a higher bentonite content (40% dry mass of bentonite) in the NSC Experiment (de La Vaissiere & Talandier 2025; Mesa-Alcantara et al. 2025). To maximize the reuse of excavated claystone for backfilling deep repository galleries and to reduce their convergence at the Meuse/Haute-Marne Underground Research Laboratory (URL), mixing crushed COx argillite and sand has also been suggested (ANDRA 2005; Leroy et al. 2024).

Therefore, drawing on diverse experimental experiences and close collaborations with various radioactive waste management agencies and IRSN, each applying different concepts and materials, this work provides an integrated view of gas-related processes in clay-based barriers. The paper compares the gas transport behavior and self-sealing capacity of these materials through hydro-mechanical testing and advanced microstructural characterization. The experimental program includes multi-scale data obtained with custom-designed equipment and test protocols tailored to the specific properties and roles of each material. The findings improve understanding of gas–liquid–soil interactions and support the development of effective sealing strategies for DGD systems. They also offer valuable insights into other geotechnical applications involving gas generation and transport, such as underground storage facilities, landfill liners, and carbon sequestration systems.

2 MATERIALS

2.1 *Host rocks*

Three different argillaceous formations were studied to represent a broad spectrum of host rock types considered in various radioactive waste disposal concepts. These include both poorly indurated and indurated clay-rich rocks, allowing for the evaluation of gas transport behavior across different depths and consistency indices (Figure 1).

2.1.1 *Plastic host rock*

Boom Clay (BC) is a poorly indurated Cenozoic clay from Mol, Belgium, proposed as a host rock for DGD. It consists mainly of kaolinite (20–30%), illite (20–30%), and smectite (10–20%), with a liquid limit of 67% and a plastic limit of 29%, classifying it as a CH (high plasticity inorganic clay). Samples were taken at a depth of 223 m at the HADES URL, with dry densities ranging from 1.66 to 1.69 Mg/m³ and degrees of saturation very close to 1 (Gonzalez-Blanco & Romero 2024). It presents a well-developed sedimentary bedding structure, which plays a key role in the hydro-mechanical and gas transport behavior. To evaluate anisotropic effects, specimens were trimmed for oedometer testing with their axes both parallel and perpendicular to the bedding planes.

2.1.2 *Indurated host rocks*

Two indurated claystones of Jurassic age were studied: Opalinus Clay (OPA) and Brown Dogger (BD), both retrieved from the Schlattingen-1 deep geothermal borehole in the Molasse Basin of Northern Switzerland. OPA is of particular interest to the Swiss DGD.

OPA originates from the Lower Dogger unit (Aalenian) and was sampled at a depth of 936 m. It contains 34–63% total clay minerals, predominantly illite (7–18%) and illite/smectite mixed layers (14–31%), along with quartz (9–40%) and calcite (11–36%) as major non-clay constituents. The samples have a dry density of 2.43 Mg/m³, a liquid limit of 29%, and a plastic limit of 18%, classifying the material as CL (low plasticity inorganic clay) (Gonzalez-Blanco et al. 2022; Senger et al. 2014; Senger et al. 2018).

Brown Dogger (BD) corresponds to the Upper Dogger unit (Bathonian/Bajocian) and was sampled at 782 m depth. It is a laminated claystone with sandy and carbonate-rich intercalations. Its clay mineral content ranges from 34% to 52%, comprising illite (10–13%), illite/smectite (16–25%), kaolinite (7–12%), and chlorite (2–4%). Non-clay phases include quartz (21–24%) and carbonates (19–33%). The BD samples showed dry densities around 2.48 Mg/m³ and degrees of saturation between 0.95 and 1.0. Based on Atterberg limits, BD falls between CL (low plasticity inorganic clay) and ML (low plasticity inorganic silt) (Gonzalez-Blanco et al. 2022; Senger et al. 2014; Senger et al. 2018).

As sedimentary shales, OPA and BD exhibit a well-defined bedding structure. Samples of both rocks were trimmed perpendicular to the bedding to assess transport behavior across planes of stratification.

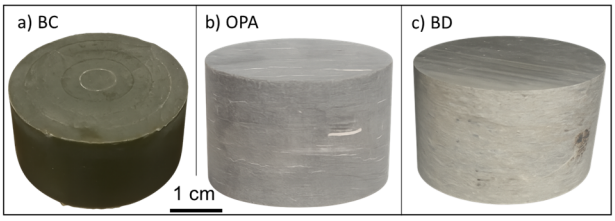

Figure 1. a) BC sample (plastic clay-rich rock at 223 m deep); b) OPA sample (indurated clay rock at 936 m); c) BD sample (indurated clay rock at 782 m).

2.2 *Engineered bentonite-based barriers/seals*

Understanding barriers and seals requires a good characterization of the hydro-mechanical properties of bentonite-based materials, the models to represent their evolution over the short term (saturation and swelling pressure) and the long term (hydrostatic increase and gas pressure increase), as well as the evolution of their homogeneity and properties during the different stages.

2.2.1 *Bentonite seals for high gas pressure*

- *Granular bentonite*

The granular bentonite (GB) studied is a sodium MX-80-type bentonite provided by NAGRA (Figure 2a). It is produced by crushing heavily compacted bentonite pellets. The as-received material, with a hygroscopic water content of approximately 7% at a relative humidity of 50%, exhibits a broad particle size distribution, including granules up to 10 mm and fine grains. It is characterized by a montmorillonite content of around 90%, a liquid limit ranging from 420% to 575%, and a plastic limit between 53% and 77%, which together confer its high swelling capacity (Zeng et al. 2023; Zeng et al. 2025).

Samples with different initial water contents were statically compacted to achieve a target dry density of ~ 1.55 Mg/m³, corresponding to the mean value measured in the Full-Scale Emplacement (FE) in situ experiment at the Mont Terri URL (Müller et al. 2017). At lower as-compacted water contents, the samples preserved a more pronounced granular structure, which gradually disappeared with increasing water content due to progressive granule disaggregation and fine-grain aggregation (Zeng et al. 2025).

- *Composite Bentonite*

The composite bentonite (CB) system studied consists of an MX-80-type bentonite mixture of 80% pellets and 20% powder provided by IRSN (Mesa-Alcantara et al. 2020; Molinero-Guerra et al. 2016). Bentonite properties are equivalent to those previously presented. The heavily anisotropic pellets were manufactured through a uniaxial compaction process, resulting in a quasi-spherical shape with a diameter of 7 mm (Laviosa-MPC, France). They showed dry densities ~ 2.06 Mg/m³ and water contents of 5–7%. During laboratory storage at a relative humidity of 50%, the pellets exhibited slight anisotropic swelling and degradation, increasing their water content to 6.1–9.4% and decreasing dry density to ~ 1.99 Mg/m³ (Mesa-Alcantara et al. 2024). The powder was produced by crushing the pellets, with a maximum particle size of 4.75 mm, water content of ~ 9.5% and a dry density of ~ 1.10 Mg/m³ (Mesa-Alcantara et al. 2020). CB samples were prepared at a dry density of 1.49 Mg/m³. Samples were assembled in layers, following a process like that of the large-scale Vertical SEALing (VSEAL) Experiment (Mokni et al. 2023). Pellets were first placed individually to achieve a high coordination number, forming a well-packed skeleton and minimizing inter-pellet voids. Once the pellet skeleton was assembled within the mold (Figure 2b), the bentonite powder was carefully added to partially fill the inter-pellet voids at a volumetric filling ratio of 61%, completing the layer preparation (Mesa-Alcantara et al. 2020).

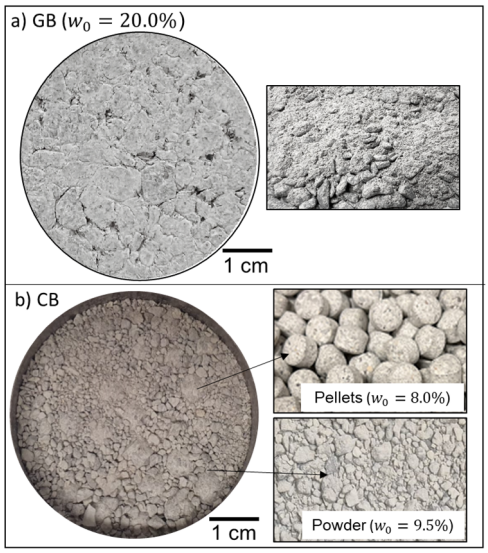

Figure 2. a) Sample of compacted GB at 1.55 Mg/m³ and water content of w_0=20% and as-received material with large granules (up to 10 mm). b) Sample of CB after pouring the powder (20% of mass) over the pellets (80%). Pictures of 7-mm pellets at w_0=8.0% and powder at w_0=9.5%.

2.2.2 *Sand/bentonite mixtures for gas-permeable seals/backfills*

NAGRA provided one of the S/B mixtures studied. It consisted of Strobel quartz sand BS650 and MX-80-type bentonite described in Section 2.2.1 in a proportion of 80/20 in mass, matching the ratio used in the GAST test (Romero et al. 2023, Romero et al. 2024). The S/B sample was dynamically compacted in layers to achieve a dry density ~ 1.64 Mg/m³ with an initial water content of 12%, ensuring that the bentonite fraction adequately filled the inter-sand pores at saturation (the initial inter-sand volumetric filling was 70%). This mixture developed swelling pressures slightly above 200 kPa, providing sufficient sealing capacity while enhancing gas permeability.

Additionally, S/B mixture with a 60/40 dry mass ratio was also investigated. This material, provided by ANDRA and linked to the NSC Experiment (de La Vaissiere & Talandier 2025), consisted of MX-80-type bentonite and quartz sand, and was delivered in the form of pre-compacted bricks with a mean dry density of 1.99 Mg/m³, reaching a swelling pressure at saturation estimated between 2.5 and 6.3 MPa. The average dry density of the bentonite in the bricks is ~ 1.45 Mg/m³. For laboratory testing, cylindrical specimens were carefully trimmed from the bricks or one-dimensionally statically compacted at high compaction stresses of around 50 MPa (Mesa-Alcantara et al. 2025).

3 EXPERIMENTAL EQUIPMENT AND PROTOCOLS

3.1 *Experimental equipment*

All tests were conducted at the Geotechnical Laboratory of Universitat Politècnica de Catalunya (UPC). For most of the materials, gas injection tests were performed using a custom-built high-pressure oedometer, isotropic, and isochoric cells designed explicitly for coupled hydro-mechanical testing. However, specialized mock-up systems were also developed, such as the mini-GAST, which replicated the dynamic layered compaction, hydration, and gas injection conditions in the GAST experiment.

3.1.1 *Oedometer, isochoric, and isotropic cells*

Different fully instrumented high-pressure oedometers (Gonzalez-Blanco et al. 2020), isotropic (Pineda et al. 2014), and isochoric (Zeng et al. 2023) cells were used for gas testing depending on the material. These apparatuses held samples with diameters of 50 mm and heights of 20-25 mm. All cells were equipped with external volume/pressure controllers for fluid injection (water and gas).

3.1.2 *Mini-GAST mock-up*

The mini-GAST mock-up was designed in-house and consists of a stainless-steel cylindrical cell with a 'barbecue' shape (500 mm in length and 300 mm in diameter and three dynamically compacted S/B layers) that allows compaction layers to remain parallel to the injected fluid pathways. The apparatus is equipped with ten lateral filters, sintered steel filters for liquid/gas injection, local load cells and pore pressure transducers, and stress/displacement-controlled mobile lids for applying initial compaction stresses and simulating constant volume boundary conditions during hydration and gas injection stages (Romero et al. 2023; Romero et al. 2024).

3.2 *Testing protocols*

3.2.1 *Hydro-mechanical stages before gas injection*

Before gas injection, distinct hydro-mechanical paths were applied depending on the material and the specific objectives of each test.

For clayey rocks, an initial pre-conditioning stage was performed to ensure that the stress state of the samples matched the in situ condition (Gonzalez-Blanco et al. 2025). Samples were loaded to their target total stress equivalent to in situ geostatic stresses and then soaked under oedometer conditions for BC or isotropic conditions for OPA and BD. Subsequently, water back-pressure saturation was applied to establish effective stresses representative of repository conditions (Gonzalez-Blanco et al. 2022).

For GB and CB materials, gas injection experiments were carried out under both unsaturated and saturated conditions, using isochoric cells for the former and stress-controlled oedometer cells for the latter. In both configurations, water was

injected by imposing a back-pressure while controlling the injected volume to reach the target degree of saturation. During this process, swelling pressure development was monitored for unsaturated samples, whereas in the oedometer tests, vertical stress was applied to counteract swelling and maintain the target sample height (Gonzalez-Blanco et al. 2020; Mesa-Alcantara et al. 2023; Zeng et al. 2023).

For the S/B mock-up test, following installation by dynamic compaction layer by layer, saturation was achieved through pressure-controlled water injection at low rates, enabling progressive hydration without inducing hydraulic fracturing or structural disturbance (Romero et al. 2023).

3.2.2 *Gas injection stages*

After confirming partial or complete saturation, gas injection tests were conducted to assess gas transport properties. Nitrogen, helium, or air served as testing gases. For BC, OPA, and BD samples, gas was injected at controlled volumetric rates—either fast (100 mL/min) or slow (<2 mL/min)—under constant vertical (oedometer conditions) or isotropic stress until reaching a maximum gas pressure below the minor principal stress. Next, the gas pump was stopped at a constant volume in the upstream reservoir, and gas pressure decay alongside outflow volume was recorded after breakthrough. Gas permeability was calculated during the dissipation phase using the generalized Darcy's law for compressible fluids over the entire sample area (e.g., Gonzalez-Blanco & Romero 2024; Pineda et al. 2014). The effective permeability to gas (product of intrinsic and relative permeability) was used because it reflects the material's ability to flow in the presence of liquid, regardless of fluid properties, especially since the degrees of saturation were not precisely known during the steady-state dissipation. Throughout the tests, axial displacements were continuously monitored to measure deformation behaviors such as dilation or compression associated with gas flow through pressure-induced pathways. Variables like gas injection rate, stress state, and bedding orientation were analyzed to understand gas transport mechanisms (Gonzalez-Blanco et al. 2022; Senger et al. 2014; Senger et al. 2018).

For GB and CB materials under unsaturated conditions, a gas injection pressure was directly applied at the upstream end, with pressure decay tracked to determine effective gas permeability. Different degrees of saturation and stress conditions were tested to explore their effects on gas transport. In the S/B mock-up tests, gas was injected after full saturation at controlled slow pressure rates. Low gas breakthrough levels were observed, and measurements of effective gas permeability after breakthrough, as well as snap-off pressures (where advective gas flow was obstructed), were recorded to evaluate the gas dissipation capacity of the engineered seal.

3.2.3 *Self-sealing stages and microstructural analyses*

Re-saturation following gas transport tests were performed to evaluate the self-sealing capacity of selected materials, including BC, OPA, and S/B mixtures. This was assessed by measuring the intrinsic water permeability before and after gas injection, to quantify any recovery in hydraulic performance due to re-saturation.

Post-test microstructural analyses included micro-computed tomography (μ-CT) for 3D imaging, field emission scanning electron microscopy (FESEM) for detailed morphological observations, and mercury intrusion porosimetry (MIP) to analyze pore size distribution changes caused by gas flow or re-saturation. These results offered insights into microstructural evolution, damage mechanisms, and the effectiveness of self-sealing after gas invasion.

4 RESULTS AND DISCUSSION

4.1 *Gas transport in host rocks*

The gas injection experiments conducted on Boom Clay (BC), Opalinus Clay (OPA), and Brown Dogger (BD) revealed systematic differences in transport behavior linked to the degree of induration and confinement conditions. All materials were tested under full saturation and stress states replicating in situ effective stresses. Despite their low intrinsic permeability, gas flow occurred in all cases through localized preferential pathways once a critical gas pressure was reached (Gonzalez-Blanco et al. 2022; Senger et al. 2014).

BC, the shallowest and least indurated formation, showed the highest effective gas permeability, typically in the range of 10^{-18} m². The onset of gas flow was associated with measurable sample expansion under oedometer conditions, more significant in tests with bedding planes orthogonal to the flow. The formation's higher porosity and lower stiffness allowed for earlier pathway activation along bedding planes and greater deformation under gas pressurization.

In contrast, OPA and BD, sampled at depths exceeding 780 m, exhibited effective gas permeabilities two to three orders of magnitude lower. Despite their higher stiffness and lower void ratios, gas was still able to migrate via localized discontinuities activated by the gas injection. Expansion deformations were limited, and pathway development was more progressive. However, the response was still rate-dependent: slower injection rates allowed for more equilibrated pressure fronts and earlier detection of gas at the outlet.

Figure 3 summarizes the effective gas permeability values versus sample depth, including data from Yang (2008) on COx claystone. The plot highlights a consistent decreasing trend of gas permeability with depth, reflecting the influence of porosity. The comparative results emphasize that gas transport in argillaceous rocks is governed by a combination of intrinsic features (e.g., porosity, anisotropy) and externally imposed conditions (stresses, gas pressures, gas injection rates). While deeper, more consolidated formations delay gas breakthrough and reduce effective permeability, they do not entirely prevent gas transport under sustained pressurization.

4.2 *High gas pressure versus gas-permeable bentonite seals*

The results reveal a clear distinction in gas breakthrough pressures between the two main categories of sealing systems investigated. Engineered retention barriers, including granular bentonite (GB) and composite bentonite (CB), exhibited considerable gas breakthrough pressures, highlighting their effectiveness in resisting gas invasion (Ali et al. 2025; Gonzalez-Blanco et al. 2020; Mesa-Alcantara et al. 2023). In contrast, gas-permeable seals, specifically the sand/bentonite (S/B), showed gas breakthrough pressures typically below 0.6 MPa, demonstrating their ability to facilitate controlled gas dissipation without excessive pressure build-up (Mesa-Alcantara et al. 2025; Romero et al. 2023; Romero et al. 2024). A summary of breakthrough pressures as a function of the sand mass content, S, is shown in Figure 4 (GB and CB correspond to $S = 0$), clearly illustrating the decreasing breakthrough pressure trend with increasing sand fraction in the S/B mixture. The dashed trend should tend to a gas breakthrough pressure (gas entry value) of ~ 3 kPa for pure sand.

Figure 5 summarizes the evolution of the effective gas permeability after breakthrough, starting from saturated conditions, as a function of the sand mass content. This behavior confirms the role of dominant granular constituents in enhancing gas connectivity and permeability, consistent with the design objectives of gas-permeable engineered systems. These materials are intentionally designed with increased gas

transport capacity, at the expense of some swelling capability and increased stiffness, to maintain operational safety under gas-generating conditions. The dashed trend should tend to an effective gas permeability of ~ 1×10^{-12} m² for medium and fine/crushed sand.

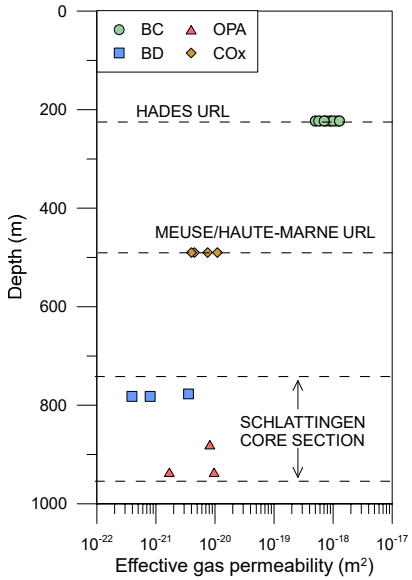

Figure 3. Effective gas permeability values after gas breakthrough starting from saturated conditions in different argillaceous host rocks.

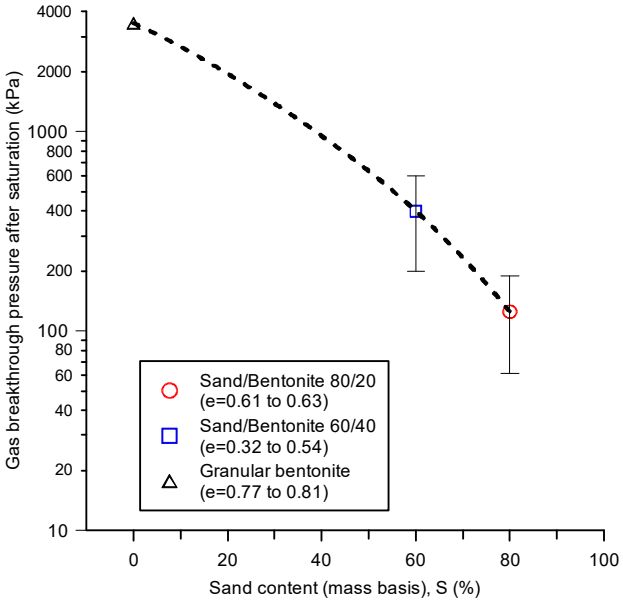

Figure 4. Gas breakthrough pressure after saturation for different sand contents in bentonite mixtures at varying void ratios.

4.3 *Self-sealing capacity after gas invasion*

Selected materials, such as BC or S/B mixtures, were subjected to re-saturation stages followed by gas transport tests to evaluate their self-sealing capacity. The intrinsic water permeability was measured before and after gas injection to quantify the potential recovery of hydraulic performance. In all cases, water permeability after re-saturation was close to the initial one, confirming the ability of these materials to self-seal gas-induced pathways and restore their sealing function (Gonzalez-Blanco et al. 2024; Romero et al. 2023). These findings reinforce the suitability of clay-based materials as long-term containment barriers in DGD systems and highlight the importance of re-saturation processes in restoring performance after gas breakthrough events.

4.4 *Microstructural changes induced by gas migration*

Post-test microstructural analyses provided valuable insights into the mechanisms of gas flow and self-sealing. For example, μ-CT imaging revealed the development of localized pathways in BC and GB samples after breakthrough, starting from saturated or nearly saturated conditions. These pathways coincided with fissures throughout or bridging bedding planes or low-density gel-like zones (Gonzalez and Romero 2024; Zeng et al. 2023). MIP results confirmed changes in the pore size distribution after gas breakthrough, with an increase in the volume of voids at the macro-scale (>2 μm). However, these macropore volumes disappeared upon re-saturation, reflecting the self-sealing capability (Gonzalez-Blanco et al 2024).

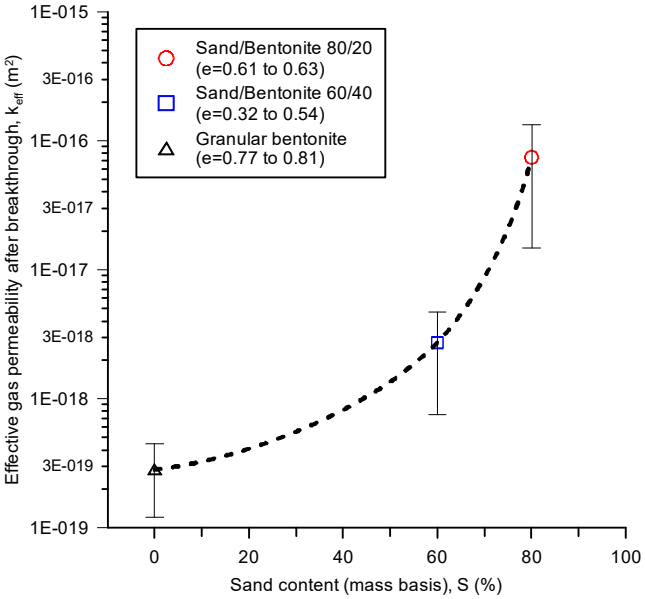

Figure 5. Gas effective permeability after breakthrough for different sand contents in bentonite mixtures at varying void ratios.

5 CONCLUSIONS

This work presents a compilation of information on understanding gas transport in clay-based materials for deep geological disposal and other gas-sensitive geotechnical applications. Using advanced testing protocols and custom-designed equipment, the Geotechnical Laboratory at the Universitat Politècnica de Catalunya (UPC) has created a solid experimental framework to explore the complex interaction between gas transport, microstructure, and hydro-mechanical boundary conditions. The results show that the material's inherent properties do not just control gas movement in low-permeability systems but are also heavily influenced by factors such as stress state and history, degree of saturation, gas pressure, and gas volumetric or pressure injection rates. In all tested materials, both natural host rocks and engineered clay-based barriers/seals, gas migration occurs through preferred pathways once specific pressures are reached, highlighting the importance of coupled analyses and careful assessment of sealing performance as conditions evolve in a repository. The laboratory's multi-scale, multi-material approach provides a valuable platform for guiding future research and collaborations in environmental and energy geotechnics.

6 ACKNOWLEDGEMENTS

The authors gratefully acknowledge the support of ANDRA, ISRN, NAGRA, and ONDRAF/NIRAS through various collaborative research projects with CIMNE. They also

sincerely appreciate financial support from the Spanish Ministry of Science and Innovation and Research Agency (MCIN/AEI/10.13039/501100011033), co-funded by the European Union (FEDER), through project PID2022-141429OB-I00 (INTERMO2, 2023–2027). Special thanks are extended to the research team at the UPC Geotechnical Laboratory for their contributions to gas-related studies, particularly Prof. A. Lloret, Dr. C. Alvarado, Dr. A. Mesa-Alcantara, Dr. J. Torres-Serra, and Dr. H. Zeng.

7 REFERENCES

Ali, M., Sanchez, M., Romero, E. et al. 2025 Experimental and numerical investigation of gas breakthrough in barrier systems for geological repositories of high-level nuclear waste. *Engineering Geology* 355, 108196. https://doi.org/10.1016/j.enggeo.2025.108196

ANDRA 2005. Evaluation of the feasibility of a geological repository in an argillaceous formation. *Dossier 2005 Argile Synthesis Report*, ANDRA.

de La Vaissiere, R. and Talandier, J. 2025. More than ten years of hydration of an in situ large-scale sealing experiment (NSC), Meuse/Haute-Marne Underground Research Laboratory, France. *Journal of Rock Mechanics and Geotechnical Engineering.* https://doi.org/10.1016/j.jrmge.2025.03.038

Gonzalez-Blanco, L., Romero, E., and Marschall, P., 2020. Gas transport in granular compacted bentonite: coupled hydro-mechanical interactions and microstructural features. *E3S Web of Conferences*, 195, 04008. https://doi.org/10.1051/e3sconf/202019504008.

Gonzalez-Blanco, L., Romero, E., Marschall, P., and Levasseur, S. 2022. Hydromechanical Response to Gas Transfer of Deep Argillaceous Host Rocks for Radioactive Waste Disposal. *Rock Mechanics and Rock Engineering*, 55(3), pp. 1159–1177. https://doi.org/10.1007/s00603-021-02717-3

Gonzalez-Blanco, L., Romero, E. and Levasseur, S. 2024. Self-Sealing of Boom Clay After Gas Transport. *Rock Mechanics and Rock Engineering* 57, 4173–4189. https://doi.org/10.1007/s00603-023-03529-3

Gonzalez-Blanco, L. and Romero, E. 2024. A multi-scale insight into gas transport in a deep Cenozoic clay. *Géotechnique*, 74(4), pp. 337–354. https://doi.org/10.1680/jgeot.21.00208

Gonzalez-Blanco, L., Llabjani, Q., Romero, E., et al. 2025. Comparative study of gas testing protocols in clayey rocks for nuclear waste repositories. *Environmental Geotechnics.* https://doi.org/10.1680/jenge.24.00185

Harrington, J.F., Graham, C.C., Cuss, R.J., and Norris, S., 2017. Gas network development in a precompacted bentonite experiment: Evidence of generation and evolution. *Applied Clay Science*, 147, pp. 80-89. https://doi.org/10.1016/j.clay.2017.07.005

Leroy, A., Cuisinier, O., Masrouri, F., and Talandier, J. 2024. Sand-claystone mixtures: Investigating the impact of sand proportions on hydro-mechanical behavior at different scales. *9th International Conference on Clays in Natural and Engineered Barriers for Radioactive Waste Confinement*, Hannover, Germany, 25-29 November 2024. https://zenodo.org/records/15072021

Levasseur, S., Collin, F., Dymitrowska, M. et al. 2024. State of the Art on Gas Transport in Clayey Materials – Update 2023. Deliverable D6.2 of the HORIZON 2020 project EURAD, Work Package Gas. EC Grant agreement no: 847593. https://www.ejp-eurad.eu/publications/eurad-d81-state-art-report

Llabjani, Q., Ferrari, A., Marschall, P., and Laloui, L. 2025. Hydro-mechanical insights for radioactive waste disposal from gas injection experiments in shale. *International Journal of Rock Mechanics and Mining Sciences*, 186, 106039. https://doi.org/10.1016/j.ijrmms.2025.106039

Marschall, P., Talandier, J., and Kolditz, O. (eds.), 2024. Barrier integrity: gas-induced impacts and model-based interpretation. EURAD-GAS: Work Package GAS (Mechanical understanding of gas transport in clay-based materials) of the HORIZON 2020 project EURAD. EC Grant agreement no: 847593. Deliverable D6.8. https://igdtp.eu/wp-content/uploads/2025/02/EURAD-D6.8-Technical-report-on-barrier-integrity.pdf.

Mesa-Alcantara, A., Romero, E., Mokni, N., Olivella, S. (2020). Microstructural and hydro-mechanical behaviour of bentonite pellets and powder mixtures. *E3S Web of Conferences 195, 04003*. https://doi.org/10.1051/e3sconf/202019504003

Mesa-Alcantara, A., Romero, E., and Mokni, N. 2023. Gas transport in a binary bentonite mixture used in sealing systems. *E3S Web of Conferences* 382, 14004. https://doi.org/10.1051/e3sconf/202338214004

Mesa-Alcantara, A., Romero, E., Torres-Serra, J., and Mokni, N. 2024. Compressibility of a binary bentonite-based mixture with particular emphasis on pellet orientation. *Applied Clay Science*, 261, 107575. https://doi.org/10.1016/j.clay.2024.107575.

Mesa-Alcantara, A., Torres-Serra, J., and Romero, E. 2025. Testing campaign on the characterisation of seal and backfill materials (bentonite/sand mixture and crushed COx/sand mixture). Ref 20091243. ANDRA Report.

Mokni, N., Cabrera, J., and Deleruyelle, F. 2023. On the installation of an in situ large-scale vertical SEALing (VSEAL) experiment on bentonite pellet-powder mixture. *Journal of Rock Mechanics and Geotechnical Engineering* 15(9), 2388-2401. https://doi.org/10.1016/j.jrmge.2023.04.008

Molinero-Guerra, A., Mokni, N., Delage, P., et al. 2016. In-depth characterisation of a mixture composed of powder/pellets MX80 bentonite. *Applied Clay Science*, 135, pp. 538–546. https://doi.org/10.1016/j.clay.2016.10.030.

Müller, H.R., Garitte, B., Vogt, T., et al. 2017. Implementation of the full-scale emplacement (FE) experiment at the Mont Terri rock laboratory. *Swiss Journal of Geosciences*, 110, pp. 287–306. https://doi.org/10.1007/978-3-319-70458-6_15.

Pineda, J., Romero, E., Alonso, E.E., and Pérez, T. 2014. A new high-pressure triaxial apparatus for inducing and tracking hydro-mechanical degradation of clayey rocks. *Geotechnical Testing Journal*, 37(6), pp. 933-947. https://doi.org/10.1520/GTJ20130163.

Romero, E., Alvarado, C., and Lloret, A. 2023. New challenges in experimental unsaturated soil mechanics. Experimental upscaling of an engineered gas-permeable seal. *E3S Web of Conferences*, 382, 05001. https://doi.org/10.1051/e3sconf/202338205001.

Romero, E., Alvarado, C., Lloret, A. et al. 2024. Mini GAST: Experimental upscaling of an engineered gas permeable seal. *9th International Conference on Clays in Natural and Engineered Barriers for Radioactive Waste Confinement*, Hannover, Germany, 25-29 November 2024. https://doi.org/10.5281/zenodo.15071883.

Rüedi, J., Teodori, S., Spillmann, T., et al. 2012. Gas-Permeable Seal Test at GTS: As-Built Report. NAGRA Technical Report NAB 12-59. Wettingen, Switzerland.

Senger, R., Romero, E., Ferrari, A., and Marschall, P. (2014). Characterization of gas flow through low-permeability claystone: laboratory experiments and two-phase flow analyses. *Geological Society*, Special Publications 400, 531-543. https://doi.org/10.1144/SP400.15

Senger. R., Romero, E., and Marschall, P. (2018). Modeling of Gas Migration Through Low-Permeability Clay Rock Using Information on Pressure and Deformation from Fast Air Injection Tests. *Transp Porous Med* 123, 563–579. https://doi.org/10.1007/s11242-017-0962-5

Villar, M.V., and Lloret, A. 2008. Influence of dry density and water content on the swelling of a compacted bentonite. *Applied Clay Science*, 39(1-2), pp. 38-49. https://doi.org/10.1016/j.clay.2007.04.007.

Yang, D. 2008. Caractérisation par la mesure de perméabilité au gaz de l'endommagement mécanique et hydrique dans l'EDZ des argilites du Callovo-Oxfordien. PhD Thesis Ecole des Mines de Paris, France. https://pastel.hal.science/pastel-00004660/

Zeng, H., Gonzalez-Blanco, L., Romero, E., and Fraccica, A. 2023. The importance of the microstructure on hydro-mechanical behaviour of compacted granular bentonite. *Applied Clay Science*, 246, 107177. https://doi.org/10.1016/j.clay.2023.107177

Zeng, H., Gonzalez-Blanco, L., and Romero, E. 2025. Particle size evolution of granular bentonite in hydro-mechanical paths. *Applied Clay Science*, accepted.